View Article Online / Journal Homepage / Table of Contents for this issue
Dynamic Article Links

CrystEngComm

Cite this: *CrystEngComm*, 2012, **14**, 374

www.rsc.org/crystengcomm

COMMUNICATION

Comparison of the relative stability of zinc and lithium-boron zeolitic imidazolate frameworks†

Raimondas Galvelis,[a] Ben Slater,[a] Anthony K. Cheetham[b] and Caroline Mellot-Draznieks*[a]

Received 8th July 2011, Accepted 14th November 2011
DOI: 10.1039/c1ce05854a

Published on 25 Hukuri 2011. Downloaded by Fail Open on 2025-05-07 15:12:10.

We show that dispersive interactions are important components in modelling zeolitic imidazolate frameworks (ZIF). Our comparative study of Zn-based and LiB-based zeolitic imidazolate frameworks reveals that, unexpectedly, both families exhibit a very similar structure-energy relationship, and exhibit a much larger energy spread than previously proposed. This finding suggests that from thermodynamic considerations, the diversity and synthesizability of LiB-based structures should be very similar to Zn-based ZIFs but very porous Zn- and LiB-ZIFs are predicted to be particularly challenging to synthesize. However, fewer unique LiB-based structure types have been synthesized thus far which suggests kinetic barriers may be more significant for LiB frameworks than Zn-based materials.

Zeolitic imidazolate frameworks constitute an important and well-documented sub-class of metal organic frameworks (MOFs). Tetrahedrally coordinated cations (usually Zn^{2+} or Co^{2+}) are linked by imidazole derivatives to create topologies that are analogous to those of aluminosilicate zeolites (Fig. 1 left).[1,2] The Zn^{2+} ions play the role of silicon and the imidazolate (Im^-) anions form bridges mimicking the role of oxygen. This new family of porous materials is attracting intense research interest due to their potential applications (*i.e.* separation,[3] storage,[4] and catalysis[5]). Access to new ZIFs topologies has been partly achieved in the zinc-based family through the judicious choice of linkers.[6] More than 105 phases with 25 distinct structure types have been reported so far for Zn-based ZIFs,[7] using as many as 16 substituted imidazolates.

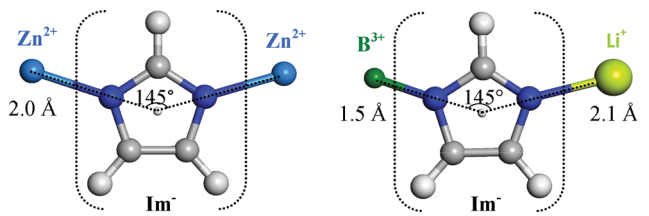

Fig. 1 Zinc-based ZIFs (left) *versus* Lithium-Boron-ZIFs (right) in terms of metal-imidazole-metal angles and distances. The centre of mass of the imidazolate linker is indicated.

A series of lightweight lithium boron analogues (also called BIFs for Boron Imidazolate Frameworks) has been reported,[8–9] wherein alternate Zn^{2+} ions are replaced by Li^+ and B^{3+}, respectively (Fig. 1 right). However, to our knowledge, only four distinct lithium-boron-based ZIF structures have been synthesized so far: two dense structures, **zni** (BIF-1) and **dia** (BIF-2),[8] and two zeotypes, **SOD** (BIF-3[8] and BIF-11[9a]) and **RHO** (BIF-9),[9b] among which only the **zni** form was obtained with unsubstituted imidazolate.

For comparison, in the case of the Zn-based ZIFs, however, the use of unsubstituted imidazolates has led to at least 8 structure types (**cag**, **BCT**, **DFT**, **GIS**, **MER**, **nog**, **zec**, and **zni**).[6] The factors causing such difference between the two families are not yet fully understood, but they are crucial for structure prediction and design of such materials.

Density Functional Theory (DFT) calculations have made significant contributions in the realm of MOFs,[10–12] and the use of a computational approach to probe the structural diversity of ZIFs is therefore of particular interest. It is becoming apparent that the inclusion of dispersive interaction corrections is crucial in DFT calculations of MOFs, for example to capture the bistability of the archetypal MIL-53 hybrid framework[13] or the mechanical properties of the dense zeolitic imidazolate **zni**.[14] This evolution in our thinking has prompted us to revisit previous DFT (without dispersive interaction corrections) studies on ZIFs, including some of our own work and that of others.[15–17]

Our motivation is that long-range dispersive interactions, which are poorly described in "standard" GGA functionals (*e.g.* leading to the exfoliation of graphite into unconnected graphene sheets), might be key to the understanding of MOFs where linker-linker interactions are known to be important. While conventional exchange–correlation functionals do not capture adequately long-range dispersive interactions,[18] several methods have been recently developed that incorporate dispersive corrections in various ways, such as a semi-empirical long range dispersive correction (DFT-D),[19,20] a non-local van der Waals functional (vdW-DF)[21] or a dispersion-corrected atom-centred potential (DCACP).[22]

Here, we utilize periodic DFT-D to evaluate the relative energies of a number of Zn-based and LiB-based ZIFs. More specifically, we probe the relative energies of a set of ZIFs topologies modelled *with*

[a]*Department of Chemistry, University College London, 20 Gordon St., London, WC1H 0AJ, UK. E-mail: c.mellot-draznieks@ucl.ac.uk*
[b]*Department of Materials Science and Metallurgy, University of Cambridge, Pembroke Street, Cambridge, CB2 3QZ, UK*
† Electronic supplementary information (ESI) available. See DOI: 10.1039/c1ce05854a

This journal is © The Royal Society of Chemistry 2012

View Article Online

Published on 25 Hukuri 2011. Downloaded by Fail Open on 2025-05-07 15:12:10.

unsubstituted imidazolate linkers. The objectives are (i) to re-evaluate the energy-density trends in both families by including dispersive interaction corrections, and (ii) to quantify the contribution of dispersive interactions. In relation to the latter issue, we have considered two variants of the semi-empirical methodology developed by Grimme and co-workers, *i.e.* DFT-D2[19] and DFT-D3.[20]

We used the experimental crystallographic data of $Zn(Im)_2$ and $LiB(Im)_4$, when available, as well as hypothetical crystal structures. In total, seven structure types (**cag**, **DFT**, **dia**, **GIS**, **MER**, **SOD**, and **zni**) have been studied for each family. For the $Zn(Im)_2$ structures, **cag** (ZIF-4),[2a] **DFT** (ZIF-3),[2a] **GIS** (ZIF-6),[2a] **MER** (ZIF-10),[2a] **SOD** (ZIF-8),[2a] and **zni**[23] are known experimentally (the crystallographic data of as-synthesized Zn–based ZIFs compounds have been retrieved from the CCDC and guest molecules eliminated, and imidazole substituent eliminated in the case of ZIF-8). $Zn(Im)_2$ **dia** frameworks has been constructed from $LiB(Im)_4$, **dia** (BIF-2)[8] by replacing Li^+ and B^{3+} cations with Zn^{2+}.

Turning to the $LiB(Im)_4$ frameworks, crystallographic data of BIF-1,[8] BIF-2,[8] and BIF-3[8] were used to derive **zni**, **dia**, and **SOD** structures, respectively. In addition, a number of hypothetical $LiB(Im)_4$ frameworks (**cag**, **DFT**, **GIS**, and **MER**) have been derived from $Zn(Im)_2$ structures by replacing Zn^{2+} cations alternately with Li^+ and B^{3+}.

The computations were performed using CP2K/Quickstep code.[24] A restricted Kohn–Sham formalism with the PBE[25] exchange–correlation functional was used. In addition, two versions of long-range dispersive interaction corrections (DFT-D2[19] and DFT-D3[20]) were evaluated. One major difference between the two approaches is that in DFT-D2, the polarisability is identical for a given atom in any chemical environment. In DFT-D3, the coordination environment of an atom is taken into account, which allows for variation in the polarisability of an atom. In addition, DFT-D3 has a more elaborate functional form (including higher order terms) and three-body terms (not used here).

Electronic energy was minimised with the orbital transformation (OT)[26] method. The convergence criterion for the self-consistent field (SCF) procedure was set to 1.0×10^{-7}. The nuclear and core electronic densities were modelled with Goedecker-Teter-Hutter (GTH)[27] pseudo-potentials and the valence electronic density represented by a mixed Gaussian and plane-wave (GPW)[28] basis sets scheme. All atoms had (molecular optimised) MOLOPT-DZVP[29] basis sets. The plane wave cut-off was set to 400 Ry. Periodic boundary conditions and Γ-point only sampling was used (the minimum simulation cell edge length was 11.3 Å). Structure optimisations were done in space group *P*1, with full relaxation of unit cell parameters and atomic positions. A summary of CP2K simulation parameters is given in Table S1.† Additionally, the impact of basis set completeness and superposition errors (BSSE) was checked with a plane-wave basis DFT code, CASTEP,[30] using PBE-D2. These calculations used the PBE functional, a cut-off of 25.7 Ry (350 eV) and sampling at the Γ-point. We considered the **MER** and **zni** structures as a benchmark.‡

Among the frameworks studied here, the **zni** structure has a special significance. Unlike others, an anhydrous framework exists in both chemical compositions (*i.e.* $Zn(Im)_2$ and $LiB(Im)_4$) with very good single crystal structure data.[8,23] This structure is also the densest polymorph known in both families. Assuming that the contribution of dispersive interactions is largest in the densest structures, the **zni** ZIFs allow us to evaluate whether the magnitude of dispersion energy to the lattice energy is significant in these materials.

Table 1 compares the experimental $Zn(Im)_2$ and $LiB(Im)_4$ **zni** structure parameters with those from DFT simulations, both without and with dispersion (PBE-D2 and PBE-D3) corrections. Including dispersion corrections greatly improves the prediction of the experimental structure (Fig. S1†), bringing the simulated values for the unit cell parameters and metal-nitrogen bond lengths into excellent agreement with experiment. The different versions of DFT-D correction perform similarly in term of accuracy in the both structures. Also, PBE-D2 calculations predicted the bulk moduli (*K*) of Zn- and LiB-**zni** in excellent agreement with the experiments, with 13.25 and 16.54 GPa for Zn-**zni** and LiB-**zni**, respectively, compared with experimental values of 14 and 16.6 GPa, respectively.[14]

Turning to the rest of the experimentally known ZIFs (Table 2), overall good agreement is observed with the crystallographic data. However, the accuracy of these simulated structures deteriorates in comparison with that of the guest-molecule free **zni** structures, probably because guest molecules present in all structures are neglected. Again DFT-D2 and DFT-D3 yield similar results. Unit cell parameters of hypothetical frameworks are given in ESI (Table S2†).

Fig. 2 shows the plots of relative energy *versus* density for $Zn(Im)_2$ and $LiB(Im)_4$ structures without (PBE) and with the dispersive interaction corrections (DFT-D2 and PBE-D3). In the absence of the corrections, the slope of energy-density trend for both $Zn(Im)_2$ and $LiB(Im)_4$ ZIFs is relatively flat and indicates a lack of energetic discrimination between different topologies, suggesting little

Table 1 Comparison of simulated and experimental $Zn(Im)_2$[23] and $LiB(Im)_4$[8] **zni** unit cell parameters and metal-nitrogen (M–N) distances, shown without (PBE) and with (PBE-D2 and PBE-D3) dispersion corrections. The relative % errors are given in parentheses. Density, *d*, is given as the number of T sites per unit volume, nm^{-3}

	a, *b*, *c* [Å]			α^a [°]	*V* [Å^3]	*d*	M–N [Å]
$Zn(Im)_2$							
Exp.	23.503	23.503	12.461	90.0	6883.1	4.65	1.99
PBE	23.942 (1.9)	23.991 (2.1)	12.660 (1.6)	90.0 (0.0)	7271.7 (5.6)	4.40 (−5.4)	2.02 (1.6)
PBE-D2	23.508 (0.0)	23.488 (−0.1)	12.468 (0.1)	90.0 (0.0)	6884.6 (0.0)	4.65 (−0.0)	2.01 (0.9)
PBE-D3	23.552 (0.2)	23.522 (0.1)	12.458 (0.0)	90.0 (0.0)	6901.5 (0.3)	4.64 (−0.3)	2.01 (0.9)
$LiB(Im)_4$							
Exp	22.504	22.504	11.515	90.0	5831.4	5.49	2.07; 1.54
PBE	22.936 (1.9)	22.936 (1.9)	11.721 (1.8)	90.0 (0.0)	6165.6 (5.7)	5.19 (−5.4)	2.11; 1.56 (1.9; 1.3)
PBE-D2	22.375 (−0.6)	22.375 (−0.6)	11.331 (−1.6)	90.0 (0.0)	5672.8 (−2.7)	5.64 (2.8)	2.06; 1.55 (−0.5; 0.2)
PBE-D3	22.410 (−0.4)	22.415 (−0.4)	11.419 (−0.8)	90.0 (0.0)	5736.1 (−1.6)	5.58 (1.7)	2.06; 1.55 (−0.7; 0.2)

[a] all structures converged towards orthorhombic cell shapes with $\alpha = \beta = \gamma$.

View Article Online

Published on 25 Hukuri 2011. Downloaded by Fail Open on 2025-05-07 15:12:10.

Table 2 Comparison of experimental (straight) and simulated (italic) $Zn(Im)_2$ unit cell parameters. The first and second lines in italic show PBE-D2 and PBE-D3 data respectively. The relative errors (%) are given in parentheses below. Density, *d*, is expressed as the number of tetrahedral T sites per unit volume, nm^{-3}.[b] For calculations on the unsubstituted imidazolate ZIF-8, see ESI

Structure	*a*, *b*, *c* [Å]			*α* [°]	*V* [Å^3]	*d*
ZIF-4 (cag)[a]	15.395	15.307	18.426	90.0	4344.9	3.68
	15.601 (*1.34*)	*14.958* (*−2.84*)	*18.086* (*−1.85*)	*90.0* (*0.00*)	*4220.3* (*−2.87*)	*3.79* (*2.95*)
	15.475 (*0.52*)	*14.958* (*−2.84*)	*18.196* (*−1.25*)	*90.0* (*0.00*)	*4211.9* (*−3.06*)	*3.80* (*3.16*)
ZIF-3 (DFT)[a]	18.970	18.970	16.740	90.0	6024.1	2.66
	19.137 (*0.88*)	*19.137* (*0.88*)	*16.867* (*0.76*)	*90.0* (*0.00*)	*6177.2* (*2.54*)	*2.60* (*−2.17*)
	19.124 (*0.81*)	*19.124* (*0.81*)	*16.837* (*0.58*)	*90.0* (*90.0*)	*6158.0* (*2.22*)	*2.59* (*−2.48*)
ZIF-6 (GIS)[a]	18.515	18.515	20.245	90.0	6940.1	2.31
	18.483 (*−0.17*)	*18.483* (*−0.17*)	*20.678* (*2.14*)	*90.0* (*0.00*)	*7064.2* (*1.79*)	*2.26* (*−1.76*)
	18.489 −(*0.14*)	*18.490* −(*0.13*)	*20.663* (*2.06*)	*90.0* (*90.0*)	*7063.8* (*1.78*)	*2.27* (*−1.75*)
ZIF-10 (MER)[a]	27.061	27.061	19.406	90.0	14210.8	2.25
	27.250 (*0.70*)	*27.250* (*0.70*)	*19.330* (*−0.39*)	*90.0* (*0.00*)	*14354.0* (*1.01*)	*2.23* (*−1.00*)
	27.239 (*0.66*)	*27.239* (*0.66*)	*19.308* −(*0.50*)	*90.0* (*90.0*)	*14326.5* (*0.81*)	*2.23* (*−0.81*)

[a] all experimental structures contain guest molecules. [b] all structures converged towards orthorhombic cell shapes with $\alpha = \beta = \gamma$.

thermodynamic obstacle to form rather open framework materials. However, when the dispersion corrections (DFT-D2 and PBE-D3) are taken into account, the slope of energy-density trend is increased significantly. This is caused by the larger contribution of the corrections to the denser frameworks in comparison to the lower density ones. This suggests that the long-range dispersive interactions are predominantly responsible of the enhanced stability of dense ZIFs, such as **zni**. It is intringuing that the variation in relative total energies of $Zn(Im)_2$ ZIFs as a function of framework density is remarkably reminiscent of that of siliceous zeolites, given the approximate 10-fold difference in density between ZIFs and zeolites.[31] We see that the **quartz/MER** energy difference is much smaller for SiO_2 than that for **zni/MER** in ZIFs, by about a factor of 2.

The different versions of the dispersive interaction correction (PBE-D2 and PBE-D3) give almost the identical relative energy orderings and densities for the both groups of frameworks. The absolute contribution of DFT-D2 is systematically larger than DFT-D3. However, it has been shown that DFT-D2 tends to overbind.[20]

Moreover, despite the different chemical composition, $Zn(Im)_2$ and $LiB(Im)_4$ ZIF structures have remarkably similar energy difference (∼30 kJ mol^{-1} per tetrahedral site) between the densest frameworks and the lightest frameworks (Fig. 3). For comparison, plane-wave energy differences at the DFT-D2 level between Zn-based **zni** and **MER** were found to be 29 kJ mol^{-1} and 31 kJ mol^{-1} for the LiB-based forms of **zni** and **MER**, confirming the veracity of the CP2K results (See ESI, Table S3 for details†).

It is noteworthy that the results of this work differ from our previous[15] work and that reported by Baburin *et al.*[16] using the PBE functional. The energy difference between the densest framework, **zni**, and the light ones (**DFT**, **GIS**, **MER**, and **SOD**) are 15–25 kJ mol^{-1} (per tetrahedral site) in the previous studies. In this study, we found the energy differences with PBE for both ZIF families are much smaller 2–5 kJ mol^{-1} (Fig. 2). In the light of the plane-wave DFT-D2 energies that compare very favourably to our GPW results here, the current study, which uses a superior basis set, with a lower basis set superposition error (BSSE) should be regarded as more accurate. Ironically, it would seem that the BSSE error inherent in our previous work on Zn-based ZIFs,[15] qualitatively captures the trend predicted by the more accurate DFT-D2 and DFT-D3 treatment.

Very recently, Baburin *et al.*[17] have published a study of the stability of LiB ZIFs where the reported energy difference between **zni** and **MER** energies was ∼20 kJ mol^{-1} (using the PBE functional). Meanwhile, the energy difference between Zn-based **zni** and **MER** frameworks (using the PBE functional) was reported to be ∼43 kJ mol^{-1}.[16] This indicates a substantial difference in the relative thermodynamic stability of Zn and LiB frameworks, in contrast to what we report here.

Our predicted trends for relative stability *versus* density for the DFT-D2 and DFT-D3 studies are essentially identical for $Zn(Im)_2$ and $LiB(Im)_4$ ZIFs. This highlights that the relative stability of a particular structure type is heavily determined by the linker interactions rather than cation-cation interactions. As a corollary, cations can be substituted preserving the structure type and the energetic trend. For example, ZIF-7 and ZIF-9 have the same **SOD** structure type and benzimidazolate linkers, but different Zn^{2+} and Co^{2+} cations, respectively. In spite of this, the frameworks have almost identical structures.[2]

Indeed, a closer analysis of Li^+, B^{3+}, and Zn^{2+} cations in their local environments, reveals that cation–nitrogen (M–N) bond lengths and partial Mulliken charges of Zn^{2+} (∼0.30) are approximately intermediate between Li^+ (∼0.46) and B^{3+} (∼−0.02). The main difference is that B–N bonds are more covalent resulting in quite short bond lengths and lower densities of LiB-based frameworks in comparison with Zn-based counterparts.

Finally, assuming that the entropic contribution is similar for a given structure type in both Zn- and LiB-based forms, from the thermodynamic point of view there is no reason why the variety of structure types is more abundant for Zn-based ZIF than LiB-based counterparts. We speculate that kinetic factors may be important. For example, the synthesis of $LiB(Im)_4$ ZIFs consist of two stages involving $[B(Im)_4]^-$ (tetraakis(imidazoly)borate) as an intermediate compound.[8–9] In contrast $Zn(Im)_2$ ZIFs are synthesized in one stage.[2]

In summary, we have shown that the dispersive interactions are important to model zeolitic imidazolate frameworks, just as it is recognised to be crucial in biological systems and molecular organic solids,[32,33] and water ices.[34] The long-range dispersive interaction correction for DFT so called DFT-D has proved to give a better description of the frameworks.

Moreover, the comparative study of $Zn(Im)_2$ and $LiB(Im)_4$ ZIFs reveals that, unexpectedly, the both families have similar relative stability trends for different topologies, while exhibiting a much larger energy spread than previously proposed with non dispersive

 This journal is © The Royal Society of Chemistry 2012

View Article Online

Published on 25 Hukuri 2011. Downloaded by Fail Open on 2025-05-07 15:12:10.

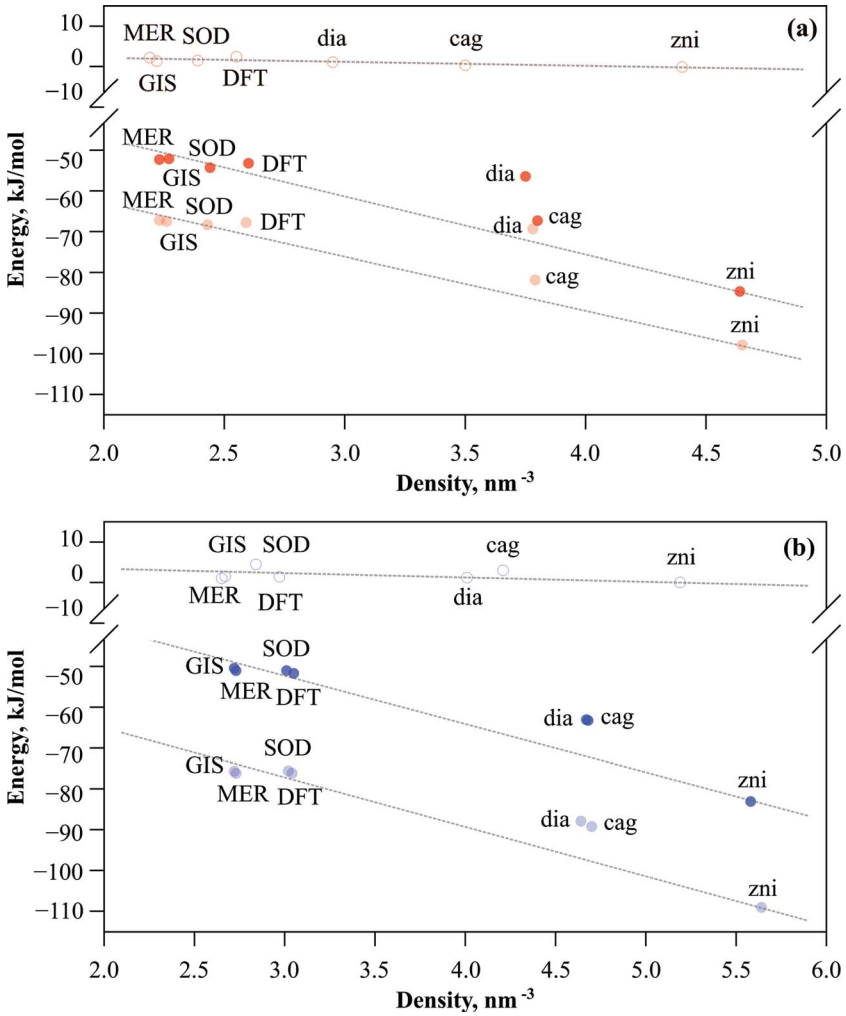

Fig. 2 Relative energies *versus* densities of $Zn(Im)_2$ (a) and $LiB(Im)_4$ (b) frameworks with PBE (empty circles), PBE-D2 (dark circles), and PBE-D3 (light circles). The relative energies are with respect to **zni** structure energy with PBE. The densities are expressed as the number of tetrahedral sites per unit volume, nm^{-3}.

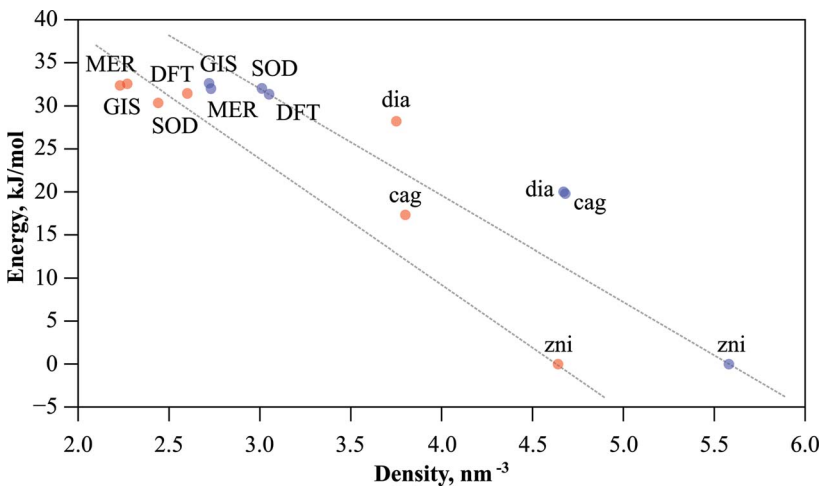

Fig. 3 Relative energies *versus* densities of $Zn(Im)_2$ (blue) and $LiB(Im)_4$ (red) ZIFs with PBE-D3. The relative energies are with respect to **zni** structure energy with the corresponding method. The densities are expressed as the number of T sites per unit volume, nm^{-3}.

View Article Online

corrected calculations. This suggests that the diversity of Zn and of LiB-based frameworks may arise from kinetic factors, which are still to be elucidated, rather than thermodynamic ones.

Acknowledgements

C.M.D. thanks the EPSRC for an Advanced Research Fellowship. A.K.C. thanks the European Research Council for an Advanced Investigator Award. We acknowledge the use of UCL computer resources and the national facility HECToR *via* our membership of UK's Materials Chemistry Consortium, which is funded by EPSRC (EP/F067496).

Published on 25 Hukuri 2011. Downloaded by Fail Open on 2025-05-07 15:12:10.

Notes and references

‡ It should be noted that both cells contain 544 atoms and therefore the computational expense of these plane wave studies is considerable and hence we considered two structures at the extrema of density.

1 Y. Q. Tian, C. X. Cai, X. M. Ren, C. Y. Duan, Y. Xu, S. Gao and X. Z. You, *Chem.–Eur. J.*, 2003, **9**, 5673.
2 (*a*) K. S. Park, Z. Ni, A. P. Côté, J. Y. Choi, R. D. Huang, F. J. Uribe-Romo, H. K. Chae, M. O'Keeffe and O. M. Yaghi, *Proc. Natl. Acad. Sci. U. S. A.*, 2006, **103**, 10186; (*b*) B. Wang, A. P. Côté, H. Furukawa and M. O'Keeffe, *Nature*, 2008, **453**, 207; (*c*) R. Banerjee, A. Phan, B. Wang, C. Knobler, H. Furukawa, M. O'Keeffe and O. M. Yaghi, *Science*, 2008, **319**, 939.
3 K. Li, D. H. Olson, J. Seidel, T. J. Emge, H. Gong, H. Zeng and J. Li, *J. Am. Chem. Soc.*, 2009, **131**, 10368.
4 R. E. Morris and P. S. Wheatley, *Angew. Chem.*, 2008, **120**, 5044–5059; R. E. Morris and P. S. Wheatley, *Angew. Chem., Int. Ed.*, 2008, **47**, 4966–4981.
5 H.-L. Jiang, B. Liu, T. Akita, M. Haruta, H. Sakurai and Q. Xu, *J. Am. Chem. Soc.*, 2009, **131**, 11302.
6 A. Phan, C. J. Doonan, F. J. Uribe-Romo, C. B. Knobler, M. O'Keeffe and O. M. Yaghi, *Acc. Chem. Res.*, 2010, **43**, 58.
7 (*a*) For a description of zeotypes symbols see: Ch. Baerlocher and L. B. McCusker, Database of Zeolite Structures: http://www.iza-structure.org/databases; (*b*) For RCSR symbols see: M. O'Keeffe, M. A. Ramsen and S. J. Yaghi, *Acc. Chem. Res.*, 2008, **41**, 1782.
8 J. Zhang, T. Wu, C. Zhou, S. M. Chen, P. Y. Feng and X. H. Bu, *Angew. Chem.*, 2009, **121**, 2580; J. Zhang, T. Wu, C. Zhou, S. M. Chen, P. Y. Feng and X. H. Bu, *Angew. Chem., Int. Ed.*, 2009, **48**, 2542.
9 (*a*) T. Wu, J. Zhang, X. Bu and P. Feng, *Chem. Mater.*, 2009, **21**, 3830; (*b*) T. Wu, J. Zhang, C. Zhou, L. Wang, X. H. Bu and P. Y. Feng, *J. Am. Chem. Soc.*, 2009, **131**, 6111.
10 H. G. Harvey, B. Slater and M. P. Attfield, *Chem.–Eur. J.*, 2004, **10**, 3270.
11 C. Lee, C. Mellot-Draznieks, B. Slater, G. Wu, W. T. A. Harrison, C. N. R. Rao and A. K. Cheetham, *Chem. Commun.*, 2006, 2687.
12 B. Civalleri, F. Napoli, Y. Noel, C. Roetti and R. Dovesi, *CrystEngComm*, 2006, **8**, 364.
13 A. M. Walker, B. Civalleri, B. Slater, C. Mellot-Draznieks, F. Cora, C. M. Zicovich-Wilson, G. Roman-Perz, J. M. Soler and J. D. Gale, *Angew. Chem., Int. Ed.*, 2010, **49**(41), 7501.
14 T. D. Bennett, J.-C. Tan, S. A. Moggach, R. Galvelis, C. Mellot-Draznieks, B. A. Reisner, A. Thirumurugan, D. R. Allan and A. K. Cheetham, *Chem.–Eur. J.*, 2010, **16**, 10684.
15 D. W. Lewis, A. R. Ruiz-Salvador, A. Gomez, L. M. Rodriguez-Albelo, F. X. Coudert, B. Slater, A. K. Cheetham and C. Mellot-Draznieks, *CrystEngComm*, 2009, **11**, 2272.
16 I. A. Baburin, S. Leoni and G. Seifert, *J. Phys. Chem. B*, 2008, **112** (31), 9437.
17 I. A. Baburin, B. Assfour, G. Seifert and S. Leoni, *Dalton Trans.*, 2011, **40**, 3796.
18 R. Lehnert and F. Seel, *Z. Anorg. Allg. Chem.*, 1980, **464**, 187.
19 S. Grimme, *J. Comput. Chem.*, 2006, **27**, 1787.
20 S. Grimme, J. Antony, S. Ehrlich and H. Krieg, *J. Chem. Phys.*, 2010, **132**, 154104.
21 D. C. Langreth, M. Dion, H. Rydberg, E. Schroder, P. Hyldgaar and B. I. Lundqvist, *Int. J. Quantum Chem.*, 2005, **101**, 599.
22 O. A. von Lilienfeld, I. Tavernelli, U. Rothlisberger and D. Sebastiani, *Phys. Rev. Lett.*, 2004, **93**, 153004.
23 V. R. Lehnert and F. Seel, *Z. Anorg. Allg. Chem.*, 1980, **464**, 187.
24 (*a*) CP2K developers page: http://cp2k.berlios.de; (*b*) J. VandeVondele, M. Krack, F. Mohamed, M. Parrinello, T. Chassaing and J. Hutter, *Comput. Phys. Commun.*, 2005, **167**, 103.
25 J. P. Perdew, K. Burke and M. Ernzerhof, *Phys. Rev. Lett.*, 1996, **77**, 3865.
26 J. VandeVondele and J. Hutter, *J. Chem. Phys.*, 2003, **118**, 4365.
27 (*a*) S. Goedecker, M. Teter and J. Hutter, *Phys. Rev. B: Condens. Matter*, 1996, **54**, 1703; (*b*) M. Krack, *Theoretica Chimica Acta*, 2005, **114**, 145.
28 G. Lippert, J. Hutter and M. Parrinello, *Molec. Phys.*, 1997, **92**, 477.
29 J. VandeVondele and J. Hutter, *J. Chem. Phys.*, 2007, **127**, 114105.
30 M. D. Segall, P. D. J. Lindan, M. J. Probert, C. J. Pickard, P. J. Hasnip, S. J. Clark and M. C. Payne, *J. Phys.: Condens. Matter*, 2002, **14**, 2717.
31 N. J. Henson, A. K. Cheetham and J. Gale, *Chem. Mater.*, 1994, **6**, 1647.
32 (*a*) S. Grimme, J. Antony, T. Schwabe and C. Mück-Lichtenfeld, *Org. Biomol. Chem.*, 2007, **5**, 741; (*b*) Y. Zhao and D. G. Truhlar, *J. Chem. Theory Comput.*, 2007, **3**, 289.
33 B. Civalleri, C. M. Zicovich-Wilson, L. Valenzano and P. Ugliengo, *CrystEngComm.*, 2008, **10**, 405.
34 B. Santra, J. Klimes, D. Alfe, A. Tkatchenko, B. Slater, A. Michaelides, R. Car and M. Scheffler, *Phys. Rev. Lett.*, 2011, **107**, 185701.

 This journal is © The Royal Society of Chemistry 2012